Title

Hydrological analysis in watersheds with a variable-resolution global climate model (VR-CESM)

Authors

Xu, Zexuan

Di Vittorio, Alan

Publication Date

2021-10-01

DOI

10.1016/j.jhydrol.2021.126646

Peer reviewed

Journal of Hydrology 601 (2021) 126646

Contents lists available at ScienceDirect

Journal of Hydrology

journal homepage: www.elsevier.com/locate/jhydrol

Research papers

Hydrological analysis in watersheds with a variable-resolution global climate model (VR-CESM)

Zexuan Xu *, Alan Di Vittorio

Climate & Ecosystem Sciences Division, Lawrence Berkeley National Laboratory, United States
Berkeley Institute for Data Science, University of California, Berkeley, United States

ARTICLE INFO

Keywords:
Watersheds
Runoff
Climate change
Global climate model
Water budget

ABSTRACT

Taditionally, watershed-scale hydrology is simulated by distributed hydrological models with offline meteorological forcing data, or by regional regional climate models that link atmospheric and land hydrology interactions. Global climate model (GCMs) are rarely used to study watershed-scale hydrology due to the relatively coarse grid resolution, computationally expensive downscaling, and simplified physical processes. Recently, however, watershed-scale hydrology analysis has become possible in GCMs due to the development of variable-resolution GCMs that dynamically couple the hydrological processes between atmospheric and land systems at fine resolutions in selected regions and coarse resolution elsewhere. In this study, we used the variable-resolution Community Earth System Model (VR-CESM) with refined-resolution (14 km) in the western U.S. and eastern China to evaluate smaller watershed-scale hydrology. We compared the historical VR-CESM outputs with gauge measurements and other hydrological models (e.g., National Water Model in the U.S.) and calibrated the subsurface runoff capacities in four mountainous watersheds. An RCP8.5 projection from 2007 to 2050 is used to estimate the impact of changing precipitation and snow climatology on watershed hydrology. We also analyzed the long-term runoff variability and the possibility of extreme runoff events as simulated by the VR-CESM. Although calibration is not possible in larger-scale watersheds, VR-CESM simulates the long-term annual variability of watersheds and provides insights on climate change impacts on hydrology. We conclude that refined-resolution VR-CESM can be used for watershed-scale hydrology analysis to understand water resources and water balance, in addition to traditional watershed-scale hydrological models. It enables hydrological analysis at multiple watersheds in one simulation and can help understand the two-way dynamics between land surface hydrology and atmospheric processes, and is especially practical for projecting climate change impacts. However, it is challenging to apply VR-CESM for hydrologic analysis in regulated watersheds as human factors (e.g., pumping, irrigation, water diversion) have not been fully addressed in VR-CESM.

1. Introduction

Multiple distributed hydrological models have been developed (e.g., ParFlow, Maxwell et al., 2009, MODFLOW, Harbaugh, 2005, SWAT Arnold et al., 2012) with numerous applications at the watershed level. These distributed hydrological models solve physically-based equations for subsurface and surface flow as well as other hydrological processes over the domain. The distributed hydrological models usually require significant efforts to set up with high-resolution input datasets, particularly for the subsurface geology and soil parameters, which may need to come from intensively-instrumented regions. The heterogeneity of data uncertainties and coverage coming from different data sources across the large-scale domain could affect the performance of hydrologic models significantly (Archfield et al., 2015). As a result, it is also structurally and computationally challenging to upscale the distributed hydrology models to larger continental or global scales. The governing equations and assumptions that are valid at fine scales may not be valid at coarser scales (Blöschl and Sivapalan, 1995), while running fine-resolution hydrological models over large regions is computationally expensive. In addition, this method captures only one-way interactions from the atmosphere to the land.

Global climate models (GCMs) have been developed to simulate Earth system processes and study various climate science questions, for example, projecting the changing climate (e.g., Massoud et al., 2019;

* Corresponding author.
E-mail address: zexuanxu@lbl.gov (Z. Xu).

https://doi.org/10.1016/j.jhydrol.2021.126646
Received 2 March 2021; Received in revised form 22 June 2021; Accepted 30 June 2021
Available online 14 July 2021

Gettelman et al., 2018; Rhoades et al., 2018), investigating the large-scale teleconnection patterns (e.g., Gettelman et al., 2018; Yuan et al., 2018), and quantifying the effects of radiation on evapotranspiration (ET) (e.g., Lian et al., 2018; Zhao et al., 2019). The applications of global climate models to evaluating watershed-level hydrology are limited and usually require additional model development, downscaling and/or postprocessing (e.g., Voisin et al., 2013; Zhou et al., 2020). The coupling of atmospheric models and lumped land surface models in GCMs generally requires simplified mechanistic hydrological processes, and most of these coupling do not include lateral flow. Most GCM simulations at present are performed at relatively coarse horizontal resolutions ($\sim 1^{\circ}$) due to the tremendous computational cost required to run them at finer resolutions. While hydrological processes have been widely investigated and have significant impacts on other earth system processes, GCMs are seldom applied to study hydrological processes because their coarse resolution inhibits reliable watershed scale analyses. Although some statistical downscaling methods have been developed and applied, these methods still have limitations such as ignoring physical principles or not being able to project novel future conditions (Maraun and Widmann, 2018; Nyunt et al., 2016; Velasquez et al., 2020). Regional climate models (RCMs) are an alternative to statistical downscaling and have been developed to run at resolutions of less than 1 km, with the flexibility of multiple nested domains at different resolutions. RCMs are driven by either coarser-resolution GCMs or reanalysis climate datasets at the outer domain, with the limitations of not simulating large-scale global circulation and the introduction of large-scale error at the RCM boundary (Xu et al., 2018; Ullrich et al., 2018). Nonetheless, simplified hydrologic processes including runoff generation, snow accumulation and snowmelt, evaporation and transpiration, and infiltration, are simulated by the land surface models in both GCMs and RCMs in order to evaluate feedbacks with the atmosphere. Given these limitations, distributed watershed-scale models are usually the preferred tools for hydrological analyses over various climate model approaches.

Offline land surface models with meteorological forcing datasets at fine resolution have also been used for hydrological analysis, but they have their limitations. For example, Li et al. (2011) evaluated the fine-resolution CLM hydrology outputs with in situ observations from the American River watershed, and concluded that the surface and subsurface runoff can appropriately simulate the monthly runoff and water budget with calibration at the watershed scale. Du et al. (2016) evaluated the hydrologic components in the CLM4 forced by both reanalysis and coupled model outputs, and reported that runoff was generally overestimated and the predictability of hydrology could be improved by addressing the compensating errors associated with precipitation and temperature. The uncertainty of this approach is partially determined by the resolution of meteorological forcing datasets and the topography and surface datasets applied in the land surface model, with additional limitations associated with coarser-resolution parameterizations being applied at finer scales. Furthermore, this approach applies to only one-way interactions from the meteorological forcing datasets to the land surface model. This means that some important feedbacks of water budgets, such as the effects of ET on vapor pressure deficit, are not simulated and may lead to uncertainties in the watershed-scale water budget computation.

Mountainous headwater watersheds are critical to water resources management in the western U.S., and the above approaches are all challenged by the complexity of this high-gradient region. The Sierra Nevada and Cascade Mountains on the west coast act as natural barriers to the dominant moisture transport pathway coming from the Pacific Ocean, and as such force condensation and store this moisture as mountain snowpack. The mountains of the Sierra Nevada provide 72% additional surface storage for irrigation and municipal use during seasonally dry summers (Dettinger and Anderson, 2015), and provide more than 60% of California's water consumption (Bales et al., 2011). Similarly, the Rocky Mountain snowpack is a primary source of water for the Colorado River basin and inland western U.S. (Serreze et al., 1999). The hydrological processes in these in forested, mountainous watersheds are usually snow-dominated and topography-driven. Understanding the interactions among forest structure, snow accumulation, snowmelt, and streamflow generation is therefore an integral component of effective water resources management (Ahl et al., 2008). Particularly, climate change will challenge current water resource management strategies due to changing resource availability in the western U.S. mountains (Hayhoe et al., 2004). Foster et al. (2016) pointed out that in snow-dominated mountain regions, climate is expected to alter two drivers of hydrology by decreasing the fraction of precipitation falling as snow and also increasing surface energy available to drive ET. In such complex regions, improving the characterization and modeling of hydrological processes is essential to better understand the hydrologic dynamics under a changing climate (He et al., 2019; Garousi-Nejad et al., 2017; Daly et al., 2017).

In this study, we demonstrate that refined-solution GCMs are applicable to perform watershed-scale hydrological analysis and alleviate some of the limitations described above. This approach is particularly novel and well-suited in projecting climate change impacts on hydrological processes and extreme events. By using a GCM with regionally-refined resolution, we leverage the two-way interactions between the atmospheric and land surface models while simulating the hydrological processes at a refined-resolution. In this paper, we analyze and evaluate hydrological simulations in four representative, unmanaged headwater watersheds in the western U.S using the variable-resolution community earth system model (VR-CESM). The methods applied in this study are described in Section 2, including the climate model experiment (Section 2.1), the runoff generation schemes and calibration approach (Section 2.2), a brief introduction of the four watersheds studied in this paper (Section 2.3), and the reference hydrological models and data (Section 2.4). The runoff calibration results are evaluated against reference models and data in Section 3.1, the application of VR-CESM to assessing climate change impacts on mean runoff is presented in Section 3.2, and the assessment of changing patterns of extreme hydrological events is presented in section (Section 3.3). VR-CESM simulations are also used to quantify the water budget in larger-scale watersheds in the western U.S. and eastern China, where grid resolution is refined at 14 km in the VR-CESM (Section 3.4).

2. Methods

2.1. Variable Resolution Global Climate Model

The technical details of VR-CESM and model evaluation were demonstrated in Xu et al. (2021), and only briefly introduced here. The VR-CESM utilizes a variable-resolution cubed-sphere grid generated by SQuadGen (Ullrich, 2014) and implemented in the Community Earth System Model, with the Community Atmospheric Model version 5 using the Spectral Element dynamical core (CAM5-SE) and the Community Land Model with Satellite Phenology version 4.0 (CLM) (Oleson et al., 2010; Lawrence et al., 2011). This study uses the FAMIPC5 (F-Atmospheric Model Intercomparison Project Component) component set, which bounds atmosphere-land coupled simulations with observationally-derived estimates of sea surface temperature and sea ice and employs well-established Atmosphere Model Intercomparison Project (AMIP) protocols with full atmospheric-land coupling and monthly prescribed ocean conditions (Ackerley et al., 2018). The monthly prescribed sea ice and sea surface temperatures (SST) are derived from a merging of the HadISST1 (Hadley Centre Sea Ice and Sea Surface Temperature dataset) and NOAA OI (National Oceanic and Atmospheric Administration Optimum Interpolation) SST datasets (Hurrell et al., 2008). The VR-CESM land topography is derived from a resolution-dependent smoothing of a global 30 arc-second elevation US Geological Survey GTOPO30 dataset using methods outlined in (Zarzycki et al., 2015). The highest-resolution surface cover dataset in

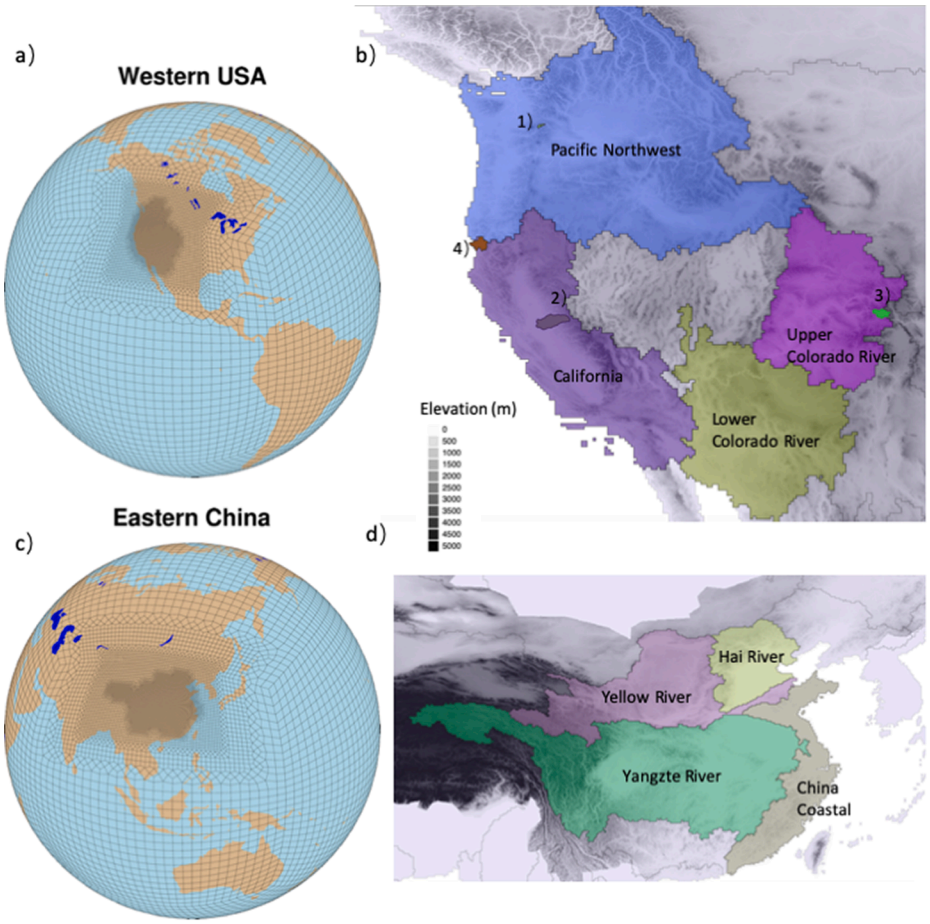

Fig. 1. (a) Refined-resolution domain in the western U.S. in the VR-CESM; (b) Four unmanaged, headwater watersheds, including American River (1), Cosumnes River (2), East-Taylor (3) and Smith River (4), and four regional-scale watersheds (California, Pacific Northwest, Upper Colorado and Lower Colorado River) at 14 km refined-resolution simulated in the VR-CESM; (c) Refined-resolution domain in the eastern China in the VR-CESM; (c) The four regional-scale watersheds (China Coastal, Hai River, Yangzte River and Yellow River) in China at 14 km refined-resolution simulated in the VR-CESM.

CLM4.0-SP, approximately 5 km resolution, was used and regridded at the same variable-resolution to produce the surface characteristics needed by VR-CESM. This particular surface cover dataset is fixed in time, derived from a composite of several satellite products, and representative of the year 2000.

Supported by an U.S. - China joint research project, the focus regions for the variable-resolution refinement include 3.12 million km^2 in the five major watersheds in the western U.S. and 4.04 million km^2 in the four major river basins in eastern China. The finest grid resolution is 14 km and covers one region in the western U.S. and one in eastern China (Fig. 1). The refined grid includes transitional buffers from 111 km grid-spacing to 55 km, 28 km, and finally 14 km over both the western U.S. and eastern China. The VR-CESM simulations span January 1969 to December 2006 for the historical simulation, and January 2007 to December 2050 for the future RCP 8.5 simulation. The first year is discarded as a spin-up period to ensure the land surface model is in equilibrium with CAM5-SE, particularly for soil moisture. The CLM initial conditions for the VR-CESM simulation are from the average of historical (1850–2006) CESM simulations and are at reasonably balanced states. Therefore, one-year spin-up is generally sufficient (Lee et al., 2015; Montavez et al., 2017), and is followed by many previous VR-CESM studies (Wu et al., 2017; Huang et al., 2016). The simulations were conducted on the Department of Energy's National Energy Research Scientific Computing Center (NERSC) Cori supercomputing system with 75 nodes (2,400 processors). The computational hour cost is ~ 43,300 h per simulation year, with 1.33 simulation years per day on Cori-Haswell.

2.2. Hydrology in CLM

CLM is the land surface model used in our VR-CESM simulation for computing runoff generation and other hydrological flux components (Oleson et al., 2010). The hydrologic cycle over land includes interception of water by plant foliage and wood, throughfall, streamflow, infiltration, runoff, soil water, and snow. These are directly linked to the biogeophysics and also affect temperature, precipitation, and runoff. Total runoff (surface and subsurface runoff) are routed downstream to oceans using a river transport model (RTM). Generally, the hydrological processes in most land surface models are over-simplified, particularly missing the lateral flow between two columns of the land surface model, and do not necessarily work best at the watershed level. However, this approach is still used in most climate models thus the assessment of its application in hydrological analyses are critical. In VR-CESM, the RTM enables the hydrologic cycle to be closed because it is synchronously coupled to CLM and routes total runoff from the land surface model to either the active ocean or marginal seas (Branstetter and Famiglietti, 1999). However, in this study the watersheds evaluated are small enough that we can use the CLM hydrology variables directly for comparison of observed and simulated streamflows on daily time scales. In addition, many other global climate models do not use RTM or have different RTM structures to route runoff through the terrain. As such, the RTM outputs are not evaluated in this paper. This also allows for more detailed analysis of surface and subsurface contributions to total streamflow and wider applicability in other models.

The runoff generation scheme in CLM is based on a simplified TOPMODEL-based representation (Niu et al., 2005), and the detailed introduction of the hydrological scheme can be found in the CLM manual (Oleson et al., 2010) and is only briefly introduced here. Both

surface and subsurface runoff are parameterized as exponential functions of the water table depth. The rate of surface runoff generation is given by

$$R_{surf} = F_{sat}p + (1 - F_{sat})max[0, (p - I)]$$

where F_{sat} is the fraction of saturated area within a grid cell, p is the effective rainfall intensity (in $mm\,s^{-1}$) (i.e., equivalent to $kg\,m^2\,s^{-1}$ in common CLM applications), which is estimated as the sum of throughfall (rainfall and dewfall after canopy interception) and snowmelt, I is the soil infiltration capacity (in $mm\,s^{-1}$), which is controlled by soil properties and soil moisture within the top soil layer. The fractional saturation area is a function of soil moisture calculated by

$$F_{sat} = F_{max}exp(-0.5f_{over}z_{\delta})$$

where F_{max} is the maximum possible saturated area fraction, f_{over} is a decay factor (m^{-1}), and z_{δ} is the water table depth (m). F_{max} is computed at 14 km resolution using the methods introduced in Tesfa et al. (2014), and the decay factor f_{over} was determined through sensitivity analysis and comparison with observed runoff to be $0.5\,m^{-1}$ (Oleson et al., 2010).

The rate of subsurface runoff generation is given by.

$$R_{sub} = R_{sb,max}exp(-f_{drai}z)$$

where $R_{sb,max}$ is the maximum subsurface runoff when the whole grid cell is saturated (in $mm\,s^{-1}$) and f_{drai} is a decay factor (m^{-1}) that represents the distribution of saturated hydraulic conductivity with depth. The total soil column in CLM is divided into 10 layers, with the thickness of each layer increasing from top to bottom. The total soil depth for hydrologic simulation is prescribed a uniform constant value of 3.802 m.

The maximum subsurface runoff values used in CLM are constant at $5.5 \times 10^{-3}\ mm\,s^{-1}$, which is derived from a sensitivity analysis of global extent. In other words, the constant values set in the model implementation are applied generally to watersheds with different actual subsurface permeability and surface conditions. Li et al. (2011) pointed out that this may lead to significant impacts on water table depth and soil moisture profile and thus influence the temporal variation of runoff generation. Li et al. (2011) performed sensitivity analysis and manual trial-and-error calibration to the default parameters in CLM, including F_{sat} and $R_{sb,max}$, in the American River watershed, and found that $R_{sb,max}$ is the major factor contributing to the unrealistically high peaks of runoff.

Following Li et al. (2011), we applied the same calibration approach to $R_{sb,max}$ using USGS gauged streamflow data measured at the outlet of each watershed. Within each watershed, $R_{sb,max}$ is assumed to be constant and calibrated against the streamflow gauge measurements at the watershed outlets. The calibration period is 1970–2006. Monthly average streamflow measurements over the calibration period (1970–2006) are used in the trial-and-error manual calibration. The calibration range of the maximum subsurface runoff $R_{sb,max}$ determined for our watersheds is set between 0 and $1.1 \times 10^{-2}\ mm\,s^{-1}$, or 0–200 % of the default maximum subsurface runoff specified in CLM. Since the calibrations are carried out independently in each of the four watersheds evaluated in this study, the resulting $R_{sb,max}$ values differ across watersheds likely due to differing hydrogeological and surface conditions. We also calibrated F_{sat} and $R_{sb,max}$ simultaneously and found that their difference is negligible in total runoff, which is similar to the results in Li et al. (2011). However, the allocation to surface and subsurface runoff can be different see Supplementary Material (1). As data are not available to validate this allocation, we take the more parsimonious approach here of calibrating only $R_{sb,max}$.

2.3. Watersheds in the western U.S.

Four unmanaged, mountainous watersheds have been selected to analyze the VR-CESM hydrological simulation (Fig. 1) to represent a wide range of geographic conditions in the western U.S. Unmanaged watersheds ideally do not have human activities such as dams, direct withdrawls, or water diversion that affect hydrological processes, and are essential for evaluation here because VR-CESM is not able to simulate these human factors. It turns out that unmanaged watersheds are usually mountainous regions with relatively small area. These four watersheds represent diverse climate and topography in the western U.S. The American River and East-Taylor River are snow-dominated watersheds, and the Cosumnes River and Smith River are rain-dominated watersheds. Watershed locations include the Pacific coast (Smith), the Sierra Nevada Mountains (Cosumnes), the Cascade Mountains (American), and the Rocky Mountains (East-Taylor). Furthermore, the American River (Li et al., 2011) and the East-Taylor River (https://watershed.lbl.gov/) are well-studied watersheds with ample data for evaluation.

The American River watershed is a mountainous watershed located along the leeward side of Mt. Rainier in the Pacific Northwest region of the U.S. The total drainage area of the American River watershed is 205 km^2, which is mainly covered by evergreen forest and shrub and underlaid by sandy soil. The elevation ranges from 850 to 2100 m. Annual precipitation in the watershed is about 1850 mm, mostly occurring in the winter season (November to January) as snowfall (Li et al., 2011).

The Cosumnes River is one of the last rivers in the Sierra Nevada region without a major dam. Thus, it offers a rare opportunity to study natural flow conditions. We should note that only the part of Cosumnes River watershed upstream of the Michigan Bar USGS station is considered here, which includes only 3500 km^2 of the total 7000 km^2 of the watershed. Above about 900 m the northern Sierra Nevada Mountains are predominately covered by a mixed evergreen forest. Spatial patterns of precipitation are highly heterogeneous across the watershed. The regional climate is considered Mediterranean with average precipitation of 1500 mm/yr, wet and cold winters with a watershed average temperature equal to 0 °C, and hot and dry summers with a watershed average temperature reaching 25 °C (Maina et al., 2020a,b).

The East-Taylor River watershed is representative of headwater catchments in the Upper Colorado Basin (Markstrom et al., 2009) with nearly 2000 km^2. The East River and Taylor River form the Gunnison River, which in turn accounts for just under half of the Colorado River's discharge at the Colorado-Utah border. The watershed has an average elevation of 3266 m, with 1420 m of topographic relief and pronounced gradients in hydrology, geomorphology, vegetation, and weather. The area is defined as having a continental, subarctic climate with long, cold winters and short, cool summers. The watershed has a mean annual temperature of 0 °C, with average minimum and maximum temperatures of −9.2 and 9.8 °C, respectively, in winter and summer seasons. The East-Taylor watershed receives an average of 1200 mm yr^{-1} of precipitation, the majority of which falls as snow (Hubbard et al., 2018).

The Smith River is the only coastal river that is evaluated in this study. It flows from the Klamath Mountains to the Pacific Ocean in Del Norte County in extreme northwestern California, on the West Coast of the United States. The river is 40.4 km long, its watershed catchment area is 1,860 km^2, without no major dams or human activities. The climate in Smith River is a typical Mediterranean regime with most precipitation falling in winter, and approximately 60% of the year's total average precipitation occurring in the four-month period from November to March. Smith River is the wettest human-inhabited spot in the state of California with the average annual precipitation amount of 1873 mm, however, very little snow falls as its daily mean temperature is moderate and ranges from 9.0 °C in February and 16.0 °C in July.

2.4. Reference hydrological models and reference datasets

The National Water Model (NWM) is a hydrologic modeling framework that simulates and forecast streamflow over the entire continental United States (CONUS). The core of the NWM system is the National Center for Atmospheric Research (NCAR)-supported community

Table 1
MAE (mean-absolute-error) for runoff simulations against USGS streamflow measurement, and the calibrated maximum subsurface runoff.

Watersheds	Historical MAE (1970–2006)		Validation MAE (2007–2019)		
	Uncalibrated	Calibrated	Uncalibrated	Calibrated	Rsub,max Value
American River	2.44	1.90	1.88	1.93	3.74×10^{-3}
Cosumnes River	1.36	0.92	1.92	1.22	1.87×10^{-3}
East-Taylor	0.96	0.54	1.22	0.63	3.74×10^{-3}
Smith River	3.75	2.74	3.63	2.63	1.87×10^{-3}

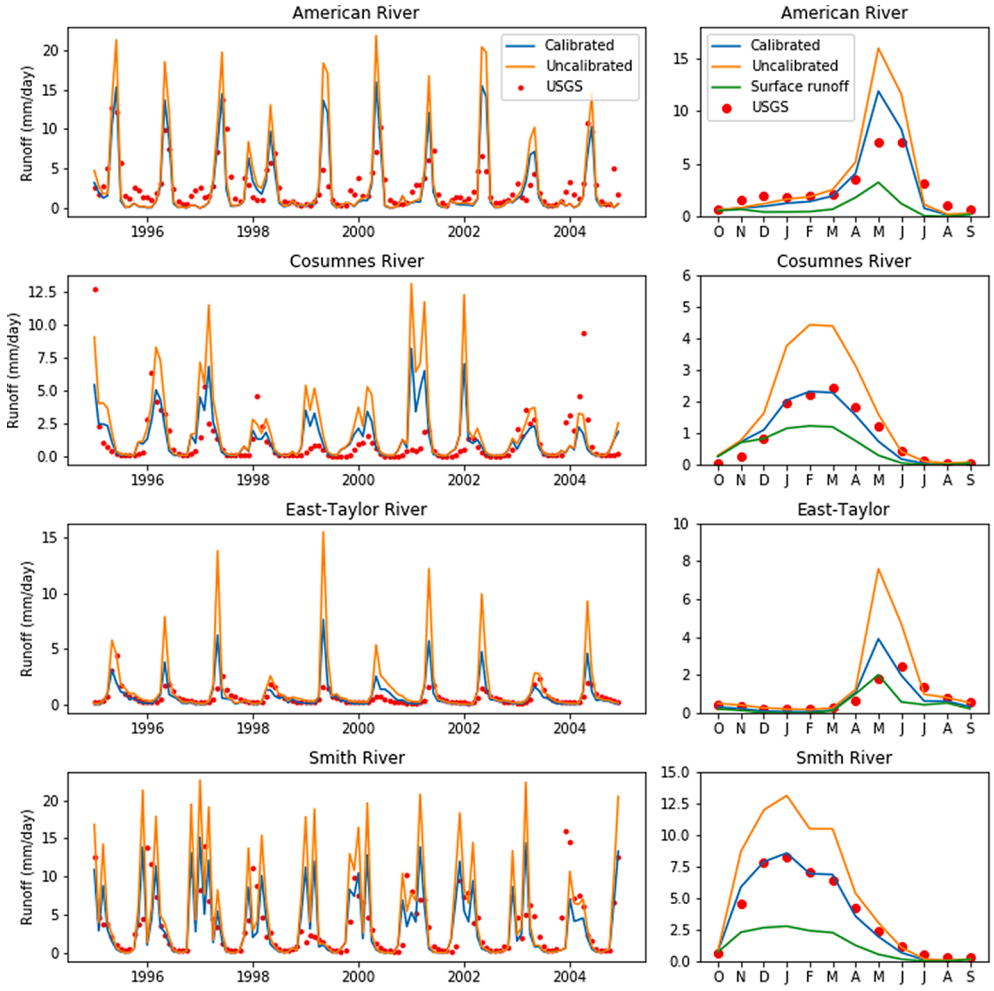

Fig. 2. Left: Calibrated and uncalibrated runoff simulation in the four watersheds in the western U.S. Left) Monthly simulated runoff and USGS gauge measurements at the watershed outlets over the last ten years of the historical period (1996–2006); Right: Monthly averaged runoff simulated runoff and USGS station measurements at the watershed outlets over the historical period (1970–2006).

Weather Research and Forecasting Hydrologic model (WRF-Hydro). It uses global forcing from a variety of sources, and is configured to use the Noah-MP Land Surface Model (LSM) to simulate land surface processes. Separate water routing modules perform diffusive wave surface routing and saturated subsurface flow routing on a 250 m grid, and routing downstream along the nriver network and output streamflow simulation at the stream reaches of the National Hydrography Dataset (NHDPlusV2). United States Geological Survey (USGS) streamflow observations are assimilated into each of the four NWM analysis and assimilation configurations and all analysis and forecast configurations benefit from the inclusion of over 5,000 reservoirs. In this study, we use the National Water Model Reanalysis dataset, which archives the model historical outputs for 25 years from 1993 to 2017, and is publicly available at https://registry.opendata.aws/nwm-archive/. NWM reanalysis dataset is selected as the reference hydrological modeling dataset in this study for model assessment, because it is one of the most widely-used operational streamflow model for at large continental scale, for example, the western U.S. It also incorporates regional climate simulation in its hydrological analyses and assimilates observations, which has the similar atmosphere-land coupling model framework compared to VR-CESM.

USGS streamflow measurements at the outlets of the four focal watersheds were used to calibrate and validate the runoff simulation in this study. The four USGS streamflow stations maintained long-term daily river discharge measurements since the beginning of our VR-CESM simulations (January 1, 1970). The USGS streamflow measurements are publicly available to be downloaded online.

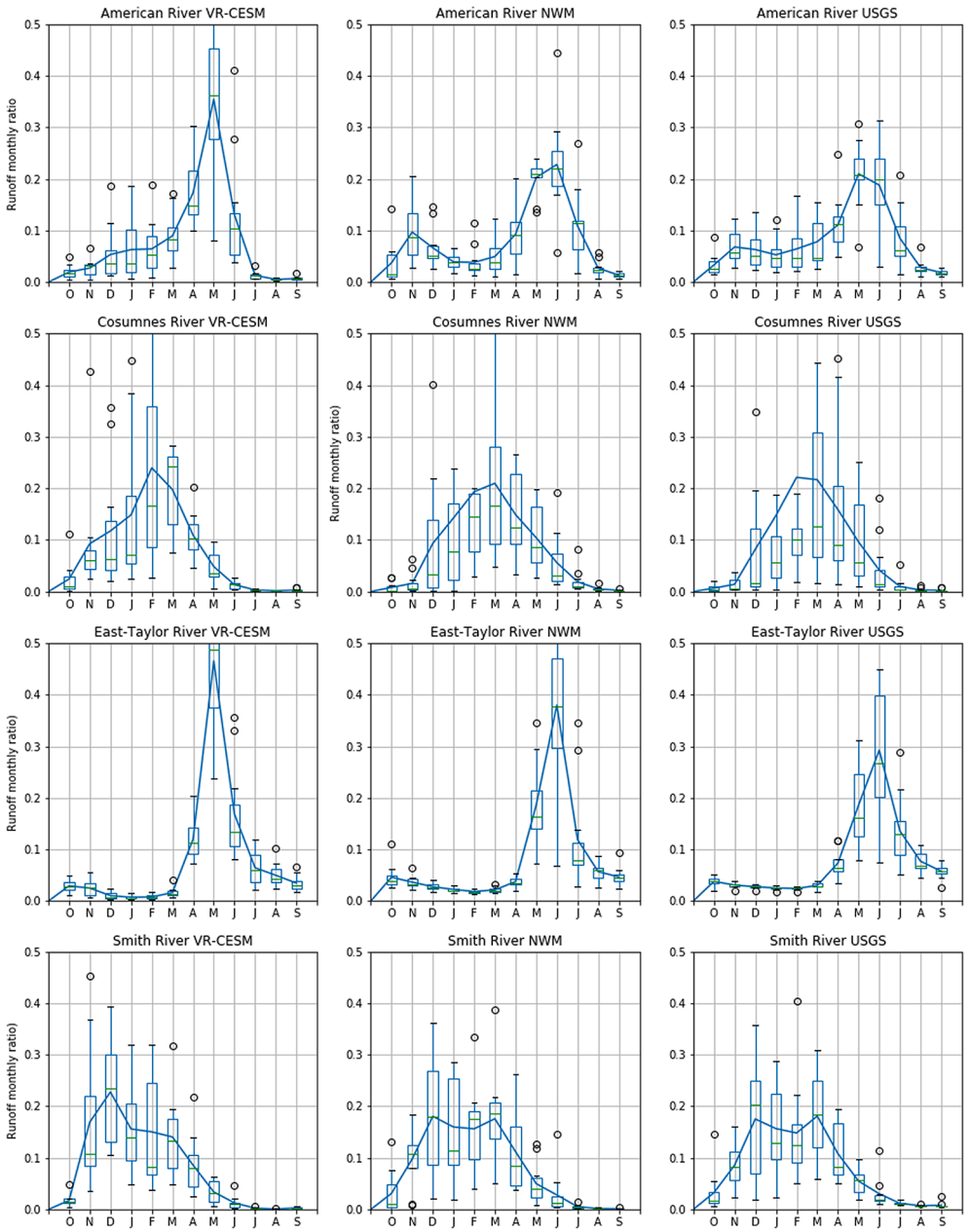

Fig. 3. Comparison of monthly calibrated runoff in VR-CESM simulation with National Water Model and USGS station measurements in the four watersheds in the western U.S. The box and whisker plot indicates the statistics of monthly climate average in the validation period (2007–2017). The National Water Model reanalysis data is only available through 2017.

3. Results

3.1. Calibration and assessments

The calibrated mean-absolute-errors (MAEs) of runoff simulations are significantly smaller than the uncalibrated runoff in comparison against USGS gauge measurements, and the maximum subsurface runoff parameter varies across watersheds. Table 1 presents the MAE of calibration and the calibrated values of ($R_{sb,max}$) for each watershed. Calibration of the maximum subsurface runoff parameter indicates that each watershed has unique geographical and climate conditions that dictate unique parameters. The MAEs at watersheds in Table 1 also indicate that the runoff calibration works better in the East-Taylor and Cosumnes River watersheds than the Smith River and American River watersheds. Fig. 2 presents the monthly calibration results for most recent 10-year period (1996–2006) in our historical simulation, and for the 37-year monthly average of calibrated and uncalibrated runoff simulations. The uncalibrated results consistently overestimate the peak of discharge whether it occurs in the winter or summer at these watersheds, while the uncalibrated and calibrated runoff are similar in the low runoff periods. The calibration particularly improves projections of peak runoff in all four watersheds, regardless of seasonal timing. In the snow-dominated American River and East-Taylor watersheds most precipitation falls in winter as snowfall that accumulates as snowpack, while the runoff peak occurs in late spring because they are high-elevation mountain watersheds significantly controlled by snow processes such as timing of snowmelt. On the other hand, runoff peaks are observed in winter in the Smith River and Cosumnes River as they are both rain-dominated watersheds located in relatively low-elevation mountains with more immediate responses to precipitation. In both cases, calibration reduces the original overestimates of these peaks. The calibrated maximum subsurface runoff values ($R_{sb,max}$) are smaller than the prescribed uniform

Table 2
Statistics of precipitation and calibrated runoff simulation in the historical (1970–2006), validation (2007–2019) and projection periods (2020–2050) in the four small watersheds in the western U.S. (American River, Cosumnes River, East-Taylor watershed and Smith River). Values in the parentheses are the ratio against historical period. Precipitation and runoff unit is mm/day.

	Historical (1970–2006)			Validation (2007–2019)			Projection (2020–2050)		
	Mean	Standard Deviation	95th Percentile	Mean	Standard Deviation	95th Percentile	Mean	Standard Deviation	95th Percentile
Precipitation American River	4.78	0.77	6.04	4.69 (0.98)	0.58 (0.74)	5.39 (0.89)	4.45 (0.93)	0.79 (1.02)	5.57 (0.92)
Cosumnes River	3.05	0.76	4.04	3.52 (1.16)	1.26 (1.66)	5.68 (1.40)	3.53 (1.16)	1.15 (1.53)	5.19 (1.28)
East-Taylor	2.60	0.35	3.26	2.83 (1.09)	0.40 (1.13)	3.55 (1.09)	2.77 (1.06)	0.38 (1.09)	3.50 (1.07)
Smith River	6.91	1.34	8.72	6.95 (1.01)	1.42 (1.06)	8.96 (1.03)	6.98 (1.01	1.74 1.30	10.75 1.23
Runoff American River	2.72	0.50	3.42	2.78 (1.02)	0.36 (0.72)	3.19 (0.93)	2.62 (0.96)	0.56 (1.14)	3.50 (1.02)
Cosumnes River	0.95	0.30	1.50	1.19 (1.25)	0.56 (1.90)	2.09 (1.40)	1.19 (1.25)	0.51 (1.71)	2.06 (1.38)
East-Taylor	0.80	0.16	1.07	0.91 (1.15)	0.16 (1.03)	1.16 (1.09)	0.85 (1.07)	0.19 (1.20)	1.14 (1.07)
Smith River	3.62	0.81	4.79	3.65 (1.01)	0.94 (1.16)	4.98 (1.04)	3.69 (1.02)	1.14 (1.41)	6.17 (1.29)

value $5.5 \times 10^{-3}\ mm\ s^{-1}$ that was determined from global data and used in the CESM simulation. Although the value of maximum subsurface runoff ($R_{sb,max}$) depends on various factors, this is consistent with physics and intuition that maximum subsurface runoff $R_{sb,max}$ is generally smaller in the mountainous regions with steeper topographical gradient than the smooth topographical regions (Li et al., 2014). We used VR-CESM to evaluate the partition of surface and subsurface runoff in the calibrated total runoff that contributes to streamflow, and found that surface runoff is nearly 30% of the total runoff in the peak runoff season, indicating that approximately 70% of the peak runoff comes from the

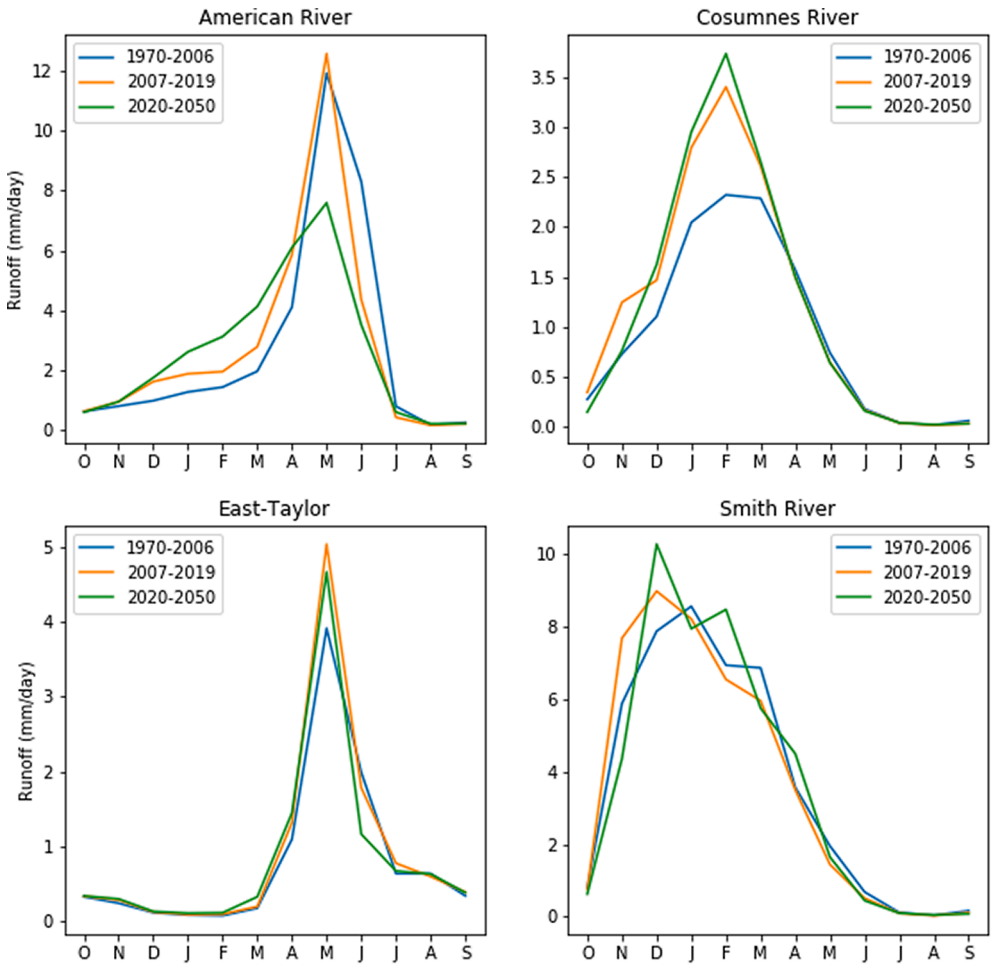

Fig. 4. Monthly calibrated runoff in the historical (1970–2006), validation (2007–2019) and projection periods (2020–2050) in the four watersheds in the western U.S.

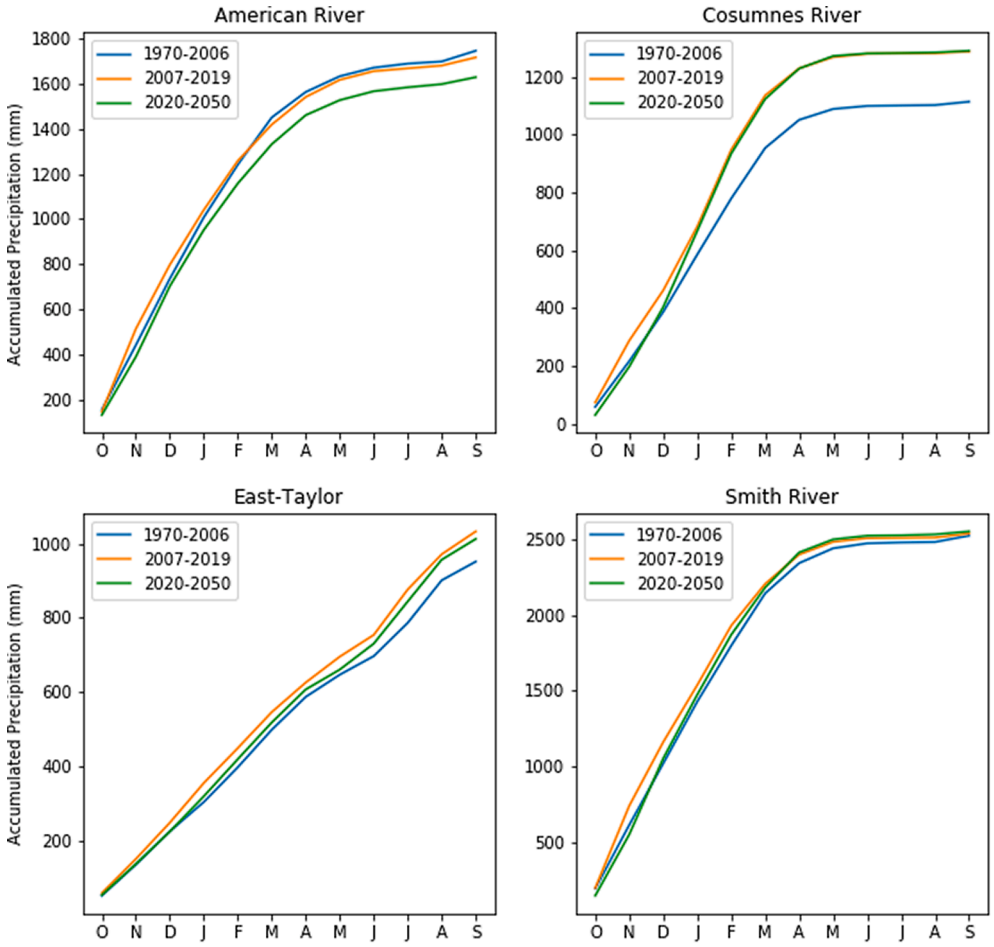

Fig. 5. Monthly accumulated precipitation in the historical (1970–2006), validation (2007–2019) and projection periods (2020–2050) in the four watersheds in the western U.S.

subsurface groundwater discharge. However, this allocation changes if F_{sat} is also calibrated against streamflow measurement (Supplementary Material 1), but we are not able to determine which presents the physical processes due to lack of data of surface and subsurface runoff partition.

We validated the calibration by comparing with USGS station measurements in the validation period (2007–2019), and the National Water Model during the period that NWM reanalysis datasets are available (2007–2017). The VR-CESM biases of the monthly fraction of annual runoff vary geographically and seasonally, as shown in Fig. 3. In the snow-dominated watersheds (American River and East-Taylor River), VR-CESM consistently overestimates the peak runoff in the snowmelt season, with greater annual variability over the historical period. The peak monthly runoff in VR-CESM is nearly 5% of the total annual runoff or higher, while simulated baseflow runoff is relatively low, compared to the National Water Model and USGS station measurements. This indicates that quantifying the uncertainties in snow processes and understanding its impacts on runoff generation are the key for hydrological analysis in these snow-dominated watersheds. On the other hand, VR-CESM runoff simulation has less difference in the rain-dominated Cosumnes River and Smith River watersheds. The peak runoff in VR-CESM is similar to that of the National Water Model and the USGS measurement, at about 2–3% of the total annual runoff. Overall, VR-CESM biases generally decrease as the amount of monthly runoff decreases. In general, the timing and magnitude of runoff are appropriately simulated in VR-CESM with the assessment of NWM and USGS station measurements. Further analyses presented in this paper are based on our calibrated version of the model, unless otherwise noted. Overall, the calibrated runoff matches reasonably well with the USGS station measurements in the validation period, particularly in the baseflow estimation. We also observed that the runoff spikes have larger uncertainties, and are overestimated in the snow-dominated watersheds.

3.2. *Assessments of climate change impacts on total runoff through 2050*

The potential impacts of climate change on hydrology vary across watersheds, likely due to their varied geographies and climate patterns. Table 2 indicates that the mean annual runoff in the American and Smith Rivers remains stable during all periods, but 7–15% and 25% increases are observed in the East-Taylor and Cosumnes River watersheds, respectively, when comparing the projection (2020–2050) and validation (2007–2019) periods against the historical period (1970–2006). In addition to the increasing trend of mean annual average runoff, the timing and magnitude of peak monthly average daily runoff in these watersheds can also vary over time. For example, peak runoff increases in the rain-dominated Cosumnes and Smith River watersheds, and decreases or stays similar in snow-dominated American and East-Taylor River watersheds (Fig. 4). In contrast to the historical period, projection period peak runoff in the rain-dominated watersheds increases approximately 20% in Smith River and as high as 60% in the Cosumnes River, suggesting that the increasing runoff in the projection period is mostly added in the peak and thus increases risk of flooding in the future. These peaks are also more pronounced in the future and shift forward one month in the Smith River. On the other hand, the peak runoff is observed in late spring and decreases nearly 30% in the snow-

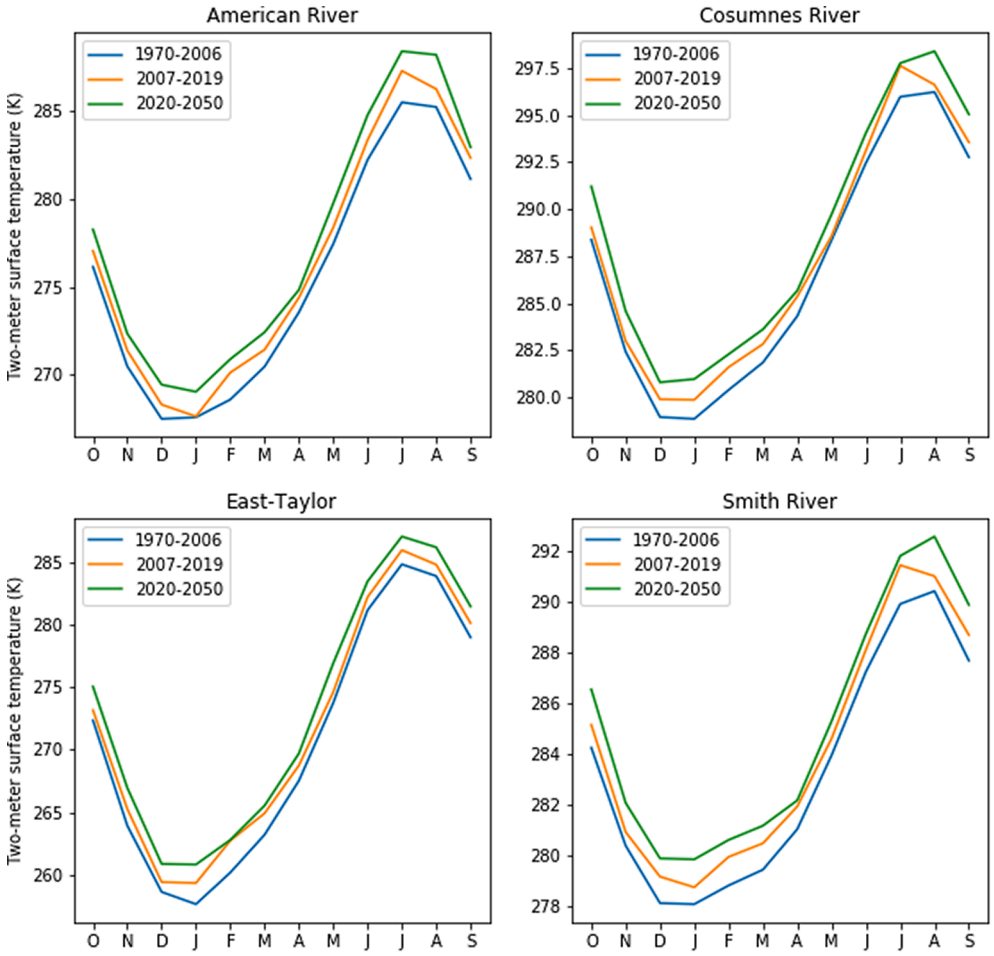

Fig. 6. Monthly two-meter surface temperature in the historical (1970–2006), validation (2007–2019) and projection periods (2020–2050) in the four watersheds in the western U.S.

dominated American River, while winter baseflow increases significantly in the projection period, potentially due to smaller snow/rain ratios and higher snowmelt. Compared to other watersheds, a smaller increase in peak runoff is simulated in the East-Taylor watershed between the historical and projection periods, as a result of changing temperature impacts on precipitation and snow.

To better understand the differences in runoff generation across these watersheds, we further evaluate potential climate change impacts on precipitation and snow. Correlation coefficients between calibrated runoff simulation and meteorological variables (precipitation, snow water equivalent and daily average temperature) with lags from 0 to 11 months are computed to help quantitative analysis of the causes of runoff changes (Supplementary Material 2). The change of precipitation between the historical and projection periods varies among watersheds. Table 2 shows that daily average precipitation slightly decreases 7% in American River and remains the same in Smith River, but increases approximately 6% in the East-Taylor watershed and 16% in the Cosumnes River watershed. Fig. 5 shows the simulated accumulated precipitation in the four watersheds during the historical, validation and projection periods, although the detailed discussion of changing precipitation is beyond the scope of this paper. These annual changes are due mainly to seasonally dependent changes in the magnitude of monthly precipitation and vary among watersheds. Precipitation increases mostly during summer in the East-Taylor watershed in Colorado, likely due to summer thunderstorms (Hubbard et al., 2018; Carroll et al., 2020). As a result, increasing precipitation does not change the magnitude of runoff peaks in the late spring and early summer in the East-Taylor watershed. Uniquely, East-Taylor watershed in the Upper Colorado River has similar average monthly precipitation year round because it is jointly affected by water vapor from the Pacific and the summer monsoon coming from the Gulf of Mexico (Hubbard et al., 2018; Carroll et al., 2020). On the other hand, significantly increasing precipitation in the winter and spring rainy season is found in the Cosumnes River that partially contributes to the higher simulated runoff from January to April in the projection period. In the American watershed, the decrease in precipitation also occurs in winter, which may contribute to less snowpack, less summer snowmelt, and a lower peak spring runoff.

Temperature plays an important role in the amount and type of precipitation, the ratios between rain and snow, and can significantly affect the magnitude and timing of runoff at different geographical locations. Different from most hydrological modeling and analysis studies where temperature is a forcing dataset, temperature is simulated in VR-CESM in the coupled atmosphere and land surface models. Increasing temperature in the projection period compared to the historical period is consistently observed in all four watersheds throughout the year (Fig. 6). The difference from the historical period is similar across seasons with an average increase of 1 degree in the recent validation period and an average increase of more than 2 degrees in the projection period.

Future changes in simulated snow water equivalent (SWE) (Fig. 7) are related to both the temperature increases and changes in precipitation. This leads to more dramatic SWE changes than for total precipitation, and also contributes to the projected changes in runoff (Fig. 4). The average peak historical SWE in the American River watershed is 700 mm in March and is nearly 50 % of the accumulated precipitation since the beginning of water year. During the future period this peak

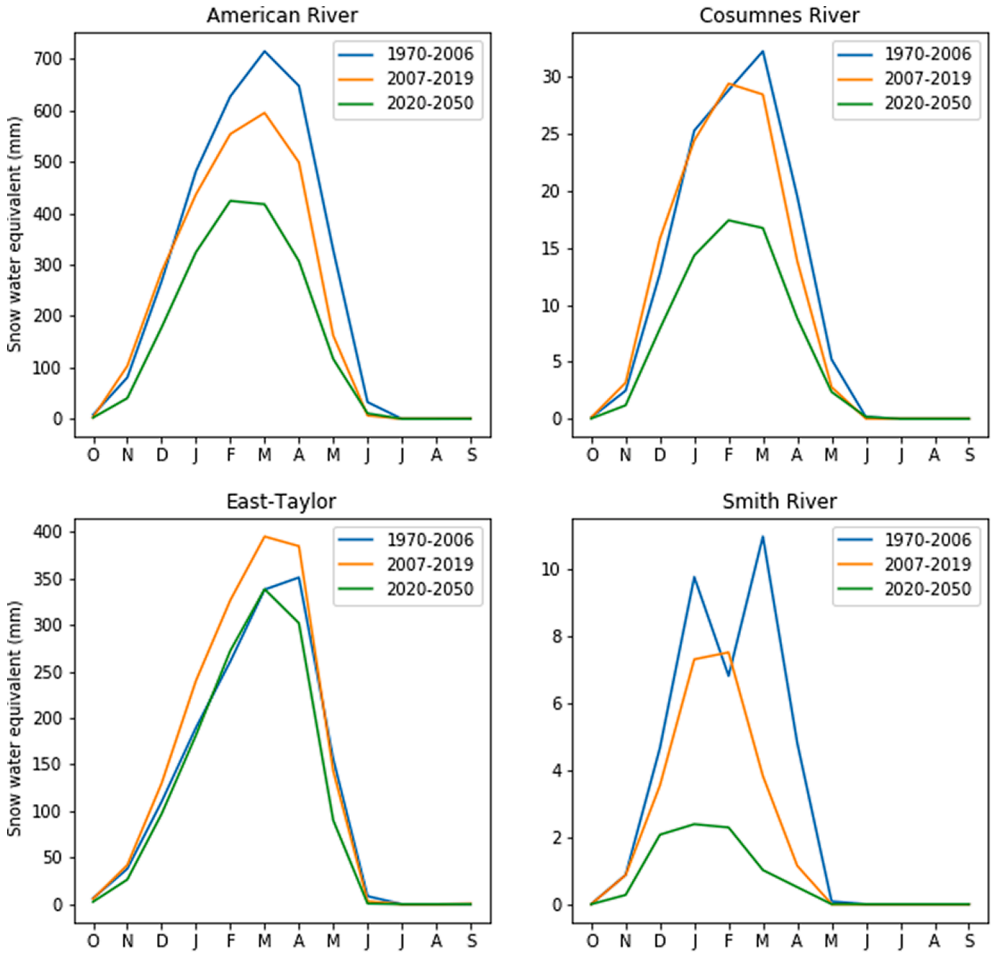

Fig. 7. Monthly snow water equivalent in the historical (1970–2006), validation (2007–2019) and projection periods (2020–2050) in the four watersheds in the western U.S.

diminishes to only 400 mm, or 28% of the accumulated precipitation, and this peak is shifted one month sooner to February. This nearly 40% SWE decrease in winter and one-month earlier start of snowmelt contribute to changes in magnitude and timing of runoff in the American watershed (Fig. 4). This indicates that climate change has significant impacts on the snow and hydrological process in the Cascade Mountain regions, where the majority of precipitation falls in winter and changing snowpack accumulation and snowmelt in spring play an important roles in runoff generation. Surprisingly, SWE is projected to be similar between the historical and future periods in the East-Taylor watershed under climate change, which has the highest elevation among all four watersheds. This has been reported by several climate projection studies (e.g., Ullrich et al., 2018; Wu et al., 2017) showing little change or even increasing SWE in high elevations because of increasing precipitation and water vapor transported from the ocean. These studies report that although temperature increases in the mountains in the projection, the daily maximum temperature still remains below freezing point so that snowpack does not melt in winter. Although SWE is not projected to decrease, warming temperatures and increased precipitation could lead to early snowmelt and thus higher runoff in the spring (Fig. 4). In the two rain-dominated watersheds, the Cosumnes and Smith Rivers, SWE is small compared to the other two watersheds and thus has less influence on streamflow, but 50–60% SWE decreases in the Cosumnes River and 80% decreases in the Smith River may still contribute to higher winter runoff peaks as precipitation may be falling as rain rather than snow (Figs. 4 and 7). The SWE peaks also shift earlier in the year for these two watersheds, which may influence runoff timing.

3.3. Extreme events

Fig. 8 shows the monthly distribution and changing temporal pattern of the 95th percentile of daily runoff (R95), a widely-used indicator of flood risk (Khomsi et al., 2016; Allen et al., 2011; Mishra and Shah, 2018). In the comparison to USGS streamflow measurements, total runoff is generally overestimated by VR-CESM during peak flow seasons. Across the watersheds, the season of highest R95 almost always coincides with the season of peak flow, for both VR-CESM and the gauge measurements refgroupFig. reffig:MonthlyTestingProjection. During non-peak flow seasons VR-CESM better estimates the R95 value, but the model doesn't always agree with the measurements on the month of peak flow as the uncertainties can be higher. For example, 95th percentile runoff at the snowmelt season from April to June are nearly 80% higher than the USGS station measurements in the American River watershed, while their differences are small during late summer and fall dry seasons. Corresponding with potential changes in runoff associated with the changing of snowfall and early snowmelt in these watersheds, future monthly R95 can be either higher or lower than the during the historical period. In both American River and Cosumnes River watersheds, the projected R95 increases approximately 30% from December to March, indicating that increasing precipitation and higher rain/snow ratio in winter could potentially amplify the risk of flooding events in winter. In American River watershed, the projected R95 decreases in May and June due to earlier snowmelt. The future R95 in East-Taylor watershed is higher than in the historical period from April to June, as East-Taylor is located at higher elevation with later snowmelt, thus shifting the risk of extreme runoff in spring. The Smith River R95 does

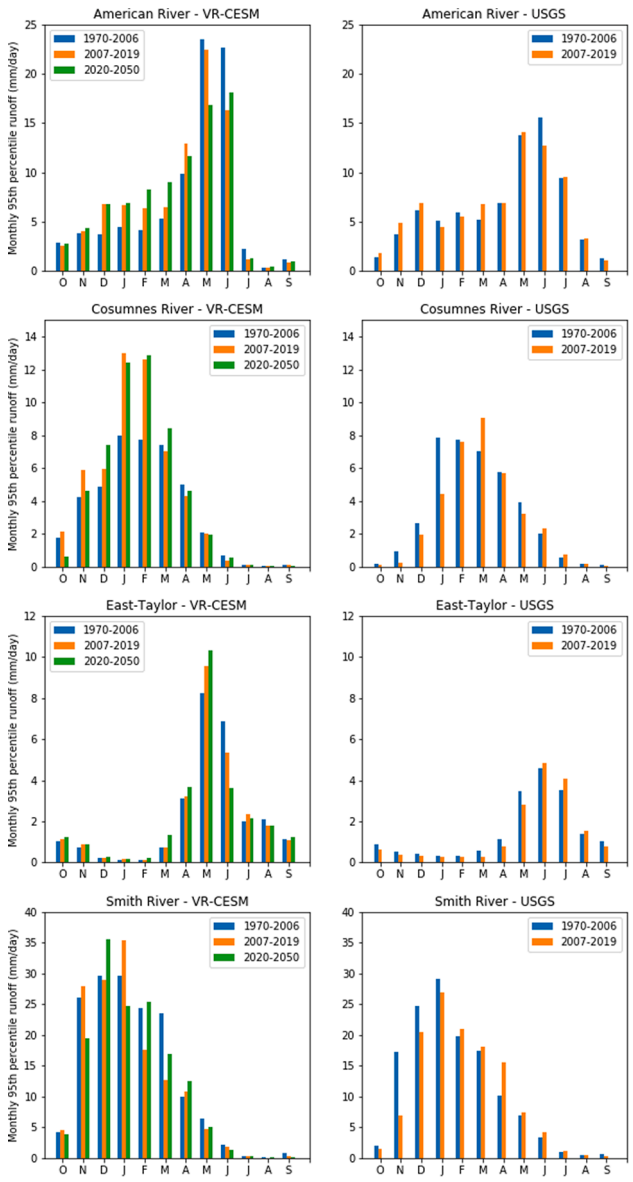

Fig. 8. Monthly 95th percentile calibrated daily runoff and USGS station measurements in the historical (1970–2006), validation (2007–2019) and projection periods (2020–2050) in the four watersheds in the western U.S.

not change much between historical and future periods likely because projected precipitation does not change significantly, and it is a rain-dominated watershed with little impact from snow. This implies that the extreme analysis of climate model and hydrological outputs are complicated and challenging, with many conditions to be considered.

Higher interannual variability of annual average daily runoff is also indicative of increases in both wet and dry extreme events. Table 2 shows that the standard deviation of annual average daily runoff increases over time in all four watersheds, with future values ranging from + 14% in the American River to as great as 71% in the Cosumnes River with respect to the historical period. Similarly, the 95th percentile of annual average daily runoff is projected to be higher in the future than during the historical period in all four watersheds. Fig. 10 presents the annual time series of the watershed budgets. Interannual variability in runoff is driven by precipitation, with ET being more stable over time. Residual values (computed as precipitation minus total runoff minus ET) indicate incomplete budget closure due to simplified model processes that do not fully account for things such as changing levels of ground water storage. For the rain-dominated watersheds, more years with extreme runoff are projected to occur during the future. The counts of extreme runoff years, defined as the annual average runoff beyond the mean + standard deviation (extreme wet) or mean - standard deviation (extreme dry) of the 37-year historical period (1970–2006), are computed in the projection period with the same 37-year interval (2014–2050) to evaluate the climate change impacts on extremes (Table 5). In the Cosumnes River watershed, the frequency of extreme wet (dry) years was estimated to be higher (lower) in the projection period compared to historical period. Similarly, in the East-Taylor river watershed, there are 7 extreme wet years in the historical period but 11 years in the projection period. In Smith River, the counts of extreme wet and dry years both increased in the projection, indicating grater inter-annual variability due to climate change. In these two watersheds, greater interannual variability and more years with extremely high annual average daily runoff are mostly relative to the similar changes in the precipitation patterns, as total runoff (subsurface runoff + surface runoff) is as large as 70–80% of the total precipitation in the water budget. On the other hand, the number of extremely high annual average daily runoff years does not change significantly in the American River watershed. The count of extreme wet (dry) years in this watershed decreases (increases) in the projection period, partially due to less precipitation. Overall, daily runoff generally shows greater future variability at monthly and annual temporal scales with changing precipitation and snow, indicating the potential for increased occurrence of extreme events and dry and wet years.

3.4. Regional-scale watersheds water budget

To assess more regional-scale hydrological projects, we looked at the annual average daily water budget components (Fig. 9) of the four USGS HUC (Hydrological Unit Code) 2 level watersheds in the western U.S.: the California, Pacific Northwest, Upper Colorado and Lower Colorado River watersheds (Fig. 1). These larger-scale watersheds are highly managed with dams, canals and pumping activities that are not simulated by VR-CESM. As a result, station measurements are not applicable for calibrating the subsurface runoff as for the smaller mountainous watersheds, nor can the previously calibrated maximum subsurface runoff values can be appropriately applied in the larger scale due to the heterogeneity of topography and soil characteristics. Therefore, the uncalibrated simulations are used in this regional-scale water budget analysis. Although runoff is overestimated, VR-CESM model outputs are still able to provide a relative estimation of each component in the water budget and evaluate climate change impacts.

Table 3 shows increasing annual average daily runoff over time in most of the western U.S., except for relatively little change in the Pacific Northwest. A majority of precipitation becomes ET in the Upper and Lower Colorado River watersheds, while ET is only approximately 30% in the Pacific Northwest and California watersheds overall. As more precipitation goes to runoff in the California and Pacific Northwest watersheds, and the precipitation variability increases in the future, these two watersheds show greater variability in runoff in the future, with the standard deviation of annual average daily runoff increasing 82% and 16%, respectively, in between the historical and projection periods (Table 3). With respect to the 95th percentile annual average daily runoff, there is a 47% increase in California and 32% increase in the Lower Colorado between the historical and future periods, but little chanege in the other two watersheds between these periods (Table 3). Similarly to the extreme analysis in the small four watersheds in the western U.S., the counts of wet and dry extreme runoff years were computed to evaluate the frequency of extreme events (Table 6). In watersheds other than the Pacific Northwest, counts of the extreme wet years are double in the projection period, while the numbers of extreme dry years are significantly decreased, compared to the historical period. Increasing frequency of extremely high annual average runoff is related to higher precipitation, for example, in the California watershed, where 18 years in the projection period are extreme wet years based on the

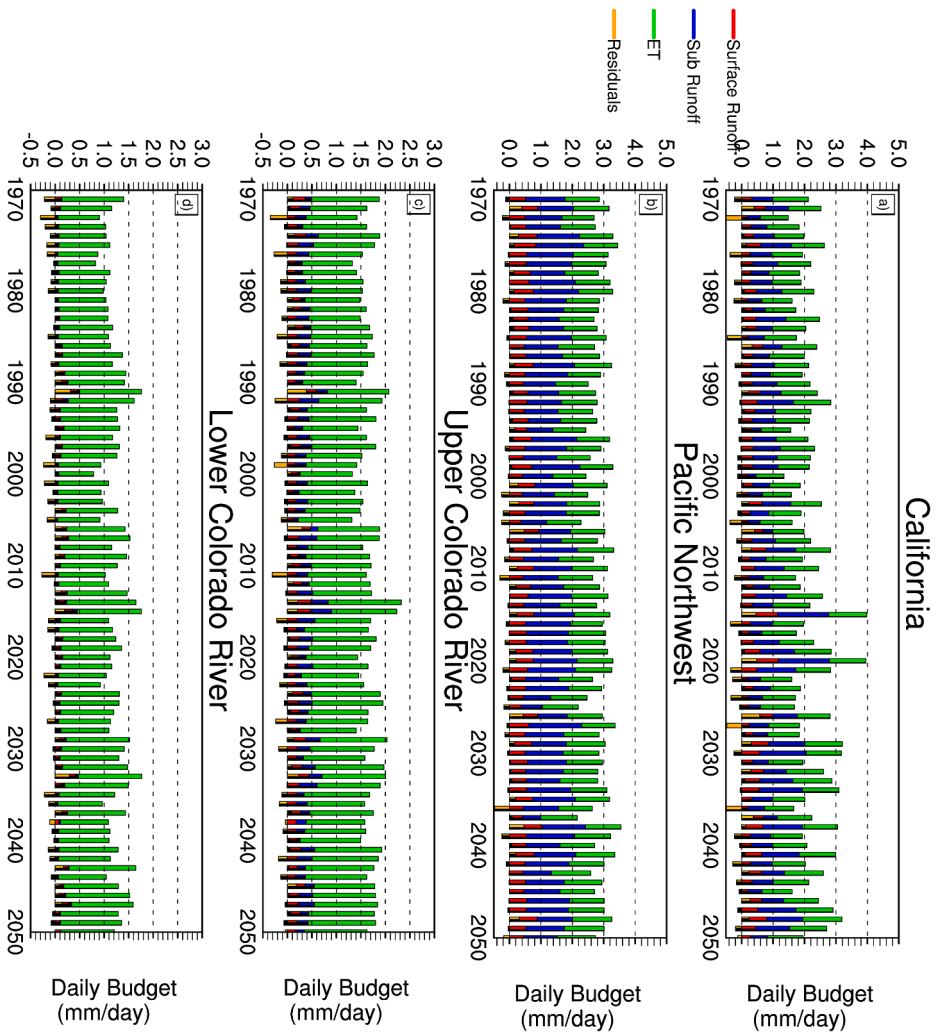

Fig. 10. Water budget of annual average precipitation, runoff and ET in the four regional-scale watersheds in western U.S (California, Pacific Northwest, Upper Colorado and Lower Colorado watersheds) from 1970 to 2050. The daily budget scale in California and Pacific Northwest are different from Lower and Upper Colorado River. Residual = Precipitation - Runoff - ET.

Table 5
Count of extreme runoff years in the four small watersheds in the western U.S. (American River, Cosumnes River, East-Taylor watershed and Smith River). Extreme runoff years are defined as the annual average runoff beyond the mean + standard deviation (extreme wet) or mean - standard deviation (extreme dry) of the 37-year historical period (1970–2006). Note that the range of projection period is redefined here to keep the same interval as the historical period.

	Historical (1970–2006)		Projection (2013–2050)	
Watersheds	Wet	Dry	Wet	Dry
American River	7	4	2	5
Cosumnes River	8	7	15	3
East-Taylor	7	2	11	2
Smith River	3	5	6	7

threshold defined in the historical period with only 7 extreme wet years. In the Pacific Northwest, however, there are only slight decreases in the number of extreme wet and dry years, likely because the average annual precipitation does not change much between historical and projection periods, but the variability does. This is consistent with the extreme analysis in the previous subsection and implies that the possibility of climate and hydrological extremes increases in the future in most watersheds. These increases in extremes may lead to increases in floods or droughts.

A similar analysis in four USGS HUC2-scale regions in China (China Coastal, Hai River, Yangtze River and Yellow River) shows different impacts across watersheds of projected climate change on the annual average daily water budget. Similar to the coastal watersheds in the western U.S., Table 4 indicates that annual average daily runoff increases by 33% and 18% in the China coastal and Yangtze River watersheds, respectively, between the historical and projection periods. The annual water budget presented in Fig. 11 clearly indicates that the China Coastal region and Yangtze River also have higher precipitation and ET in the projection period. In comparison with the historical period, the China Coastal region shows 91% higher standard deviation and 47% higher 95th percentile annual average daily runoff in the projection period (Table 4), indicating greater variability and higher possibility of extreme runoff events under a changing climate. Similarly to the extreme analysis in the western U.S., the China coastal, Yangzte River and Yellow River watersheds have 19, 16, and 9 extreme wet years in the projection, respectively, compared to the 6, 5 and 5 years in the historical period (Table 6). The counts of extreme dry years in these watersheds are also smaller in the projection period, indicating less potential for drought but higher possibility of flooding hazards under a changing climate. The annual variability of each water component, particularly the runoff, also increases with time in those three watersheds. Both the mean and standard deviation of annual average daily runoff and precipitation in the Hai River watershed, which has an arid

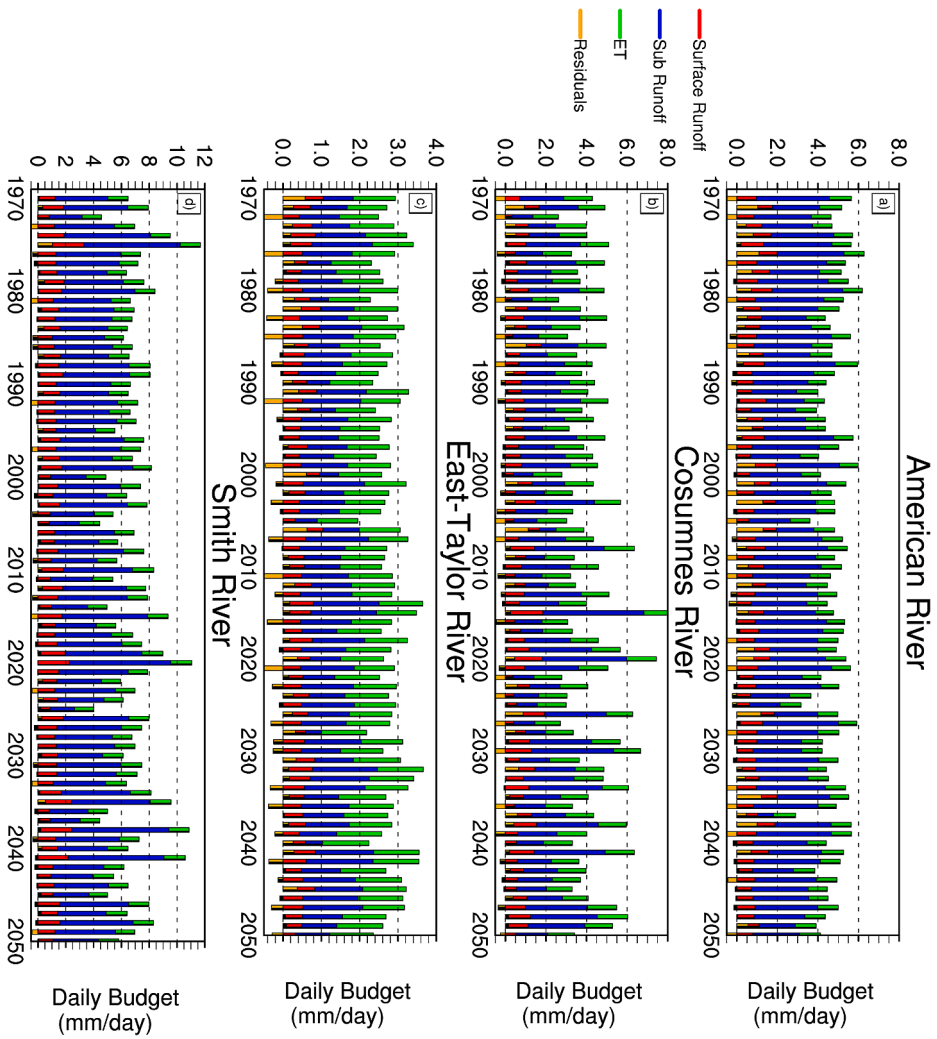

Fig. 9. Annual water budget in annual average precipitation, runoff and ET, and residual in the four mountainous watersheds in western U.S (American River, Cosumnes River, East-Taylor River and Smith River watersheds), from 1970 to 2050. Residual = Precipitation - Runoff - ET.

Table 3
Statistics of precipitation and uncalibrated runoff simulation in the historical (1970–2006), validation (2007–2019) and projection periods (2020–2050) in the four regional-scale watersheds in the western U.S. (California, Pacific Northwest, Lower Colorado and Upper Colorado watersheds). Values in the parentheses are the ratio against historical period. Unit is mm/day.

	Historical (1970–2006)			Validation (2007–2019)			Projection (2020–2050)		
	Mean	Standard Deviation	95th Percentile	Mean	Standard Deviation	95th Percentile	Mean	Standard Deviation	95th Percentile
Precipitation									
California	1.95	0.44	2.56	2.29 (1.17)	0.70 (1.59)	3.34 (1.31)	2.31 (1.18)	0.70 (1.59)	3.22 (1.26)
Pacific Northwest	2.84	0.32	3.31	2.92 (1.03)	0.28 (0.88)	3.26 (0.98)	2.87 (1.01)	0.36 (1.10)	3.33 (1.01)
Upper Colorado	1.53	0.22	1.88	1.73 (1.13)	0.29 (1.29)	2.28 (1.21)	1.67 (1.09)	0.20 (0.91)	2.00 (1.06)
Lower Colorado	1.07	0.26	1.46	1.28 (1.20)	0.30 (1.13)	1.72 (1.18)	1.22 (1.14)	0.26 (0.98)	1.65 (1.13)
Runoff									
California	0.96	0.27	1.38	1.18 (1.23)	0.47 (1.71)	1.90 (1.37)	1.21 (1.26)	0.50 (1.82)	2.03 (1.47)
Pacific Northwest	1.71	0.26	2.11	1.76 (1.03)	0.18 (0.68)	2.00 (0.95)	1.70 (1.00)	0.30 (1.16)	2.10 (0.99)
Upper Colorado	0.38	0.09	0.50	0.47 (1.23)	0.12 (1.33)	0.65 (1.31)	0.40 (1.06)	0.09 (1.05)	0.54 (1.09)
Lower Colorado	0.09	0.04	0.15	0.12 (1.31)	0.05 (1.20)	0.20 (1.38)	0.10 (1.12)	0.04 (0.93)	0.19 (1.32)

Table 6
Count of extreme runoff years in the four regional-scale watersheds in the western U.S. (California, Pacific Northwest, Lower Colorado and Upper Colorado watersheds), and four regional-scale watersheds in China (China Coastal, Hai River, Yangtze River and Yellow River watersheds). Extreme runoff years are defined as the annual average runoff beyond the mean + standard deviation (extreme wet) or mean - standard deviation (extreme dry) of the 37-year historical period (1970–2006). Note that the range of projection period is redefined here to keep the same interval as the historical period.

	Historical (1970–2006)		Projection (2013–2050)	
Watersheds	Wet	Dry	Wet	Dry
California	7	8	18	3
Pacific Northwest	8	6	7	4
Upper Colorado	6	4	15	0
Lower Colorado	6	6	14	0
China Coastal	6	7	19	3
Hai River	7	5	7	4
Yangtze River	5	6	16	4
Yellow River	5	6	9	1

climate, do not vary much with time and ET is water limited and does not increase as much as in the Yangtze River and China Coastal regions. In general, most of the watersheds in China also exhibit changes in the annual water budget due to projected climate change.

4. Conclusion

In this study, we evaluated an application of a variable-resolution global climate model (VR-CESM) in varied-size watersheds in the western U.S. The simulated runoffs for four unmanaged watersheds are calibrated against discharge measurements and compared to another hydrological model. The impacts of climate change on precipitation, snowpack and runoff, as well as extreme runoff events in those watersheds are evaluated based on historical and RCP8.5 simulations. Furthermore, we quantified the water budget components in larger-scale watersheds in the western U.S. and China and evaluated their annual variability and potential climate change impacts. Our major conclusions are listed as follows.

(1) This study demonstrates the viability of applying fine-resolution GCMs for unmanaged watershed-scale hydrological analysis with careful calibration. This is promising for future hydrological analyses that include two-way feedbacks between the atmosphere and the surface. The implication is that this approach can be used by other climate model and land surface model applications at similar resolution and scales to evaluate the hydrological response to atmospheric forcing, particularly for addressing impacts under climate change.
(2) This study used UGGS streamflow gauge measurements to quantify the uncertainties of parameterizations in the runoff generation schemes, while the uncertainties of meteorological variables were evaluated in a previous study (Xu et al., 2021). For VR-CESM, the uncertainty in total runoff was considerably reduced by calibrating the maximum subsurface runoff parameter ($R_{sb,max}$) against USGS gauge measurements.
(3) The impacts of climate change on hydrology vary in snow-dominated and rain-dominated watersheds. This is largely due to the interacting effects of changes in precipitation and temperature. In snow-dominated watersheds, decreasing snowpack and early snowmelt shifts runoff peaks earlier and reduces their magnitude (Supplementary Material 2). In the rain-dominated watersheds with increasing precipitation in the projection period, peak runoff increases in the wet season.
(4) Potential climate change also affects the magnitude of extreme runoff events. In snow-dominated watersheds, early snowmelt increases the potential for high-runoff events in spring, while in rain-dominated watersheds more intense precipitation in winter increases the potential for high-runoff events in winter. Increased variation of annual average runoff and increasing precipitation in the water budget over time also indicates the potential for more extremely dry and extremely wet periods.
(5) In regional-scale watersheds in the western U.S. and China, VR-CESM generally projects increasing precipitation and runoff through the middle of this century, particularly in the coastal watersheds that receive more moisture from the ocean. Larger interannual variability and higher frequency of wet and dry years are projected for the future for most of the watersheds, indicating that climate change could affect the occurrence of extreme hydrological events thus potentially increase the risks of arising geohazards.

The increasing number of refined-resolution and/or variable-resolution GCM applications provide significant amounts of data for evaluating the hydrological processes and investigating water budgets in watersheds. With careful calibration against observation and assessment of the uncertainties in GCM hydrological models, global models like VR-

Table 4
Statistics of precipitation and uncalibrated runoff simulation in the historical (1970–2006), validation (2007–2019) and projection periods (2020–2050) in the four regional-scale watersheds in China (China Coastal, Hai River, Yangtze River and Yellow River watersheds). Values in the parentheses are the ratio against historical period. Runoff unit is mm/day.

	Historical (1970–2006)			Validation (2007–2019)			Projection (2020–2050)		
	Mean	Standard Deviation	95th Percentile	Mean	Standard Deviation	95th Percentile	Mean	Standard Deviation	95th Percentile
Precipitation									
China Coastal	3.43	0.36	4.06	3.61 (1.05)	0.42 (1.17)	4.13 (1.02)	4.02 (1.17)	0.61 (1.70)	5.10 (1.25)
Hai River	1.86	0.30	2.32	1.94 (1.04)	0.30 (1.02)	2.33 (1.00)	1.92 (1.03)	0.27 (0.93)	2.33 (1.00)
Yangtze River	3.39	0.25	3.82	3.42 (1.01)	0.26 (1.06)	3.80 (1.00)	3.73 (1.10)	0.34 (1.40)	4.24 (1.11)
Yellow River	1.78	0.19	2.08	1.79 (1.01)	0.16 (0.85)	2.02 (0.97)	1.87 (1.05)	0.15 (0.79)	2.13 (1.02)
Runoff									
China Coastal	1.52	0.28	2.01	1.65 (1.09)	0.42 (1.47)	2.13 (1.06)	2.02 (1.33)	0.54 (1.91)	2.96 (1.47)
Hai River	0.37	0.12	0.57	0.38 (1.04)	0.11 (0.91)	0.54 (0.95)	0.34 (0.94)	0.08 (0.72)	0.52 (0.91)
Yangtze River	1.57	0.25	1.96	1.53 (0.97)	0.27 (1.06)	1.92 (0.98)	1.81 (1.15)	0.34 (1.37)	2.39 (1.22)
Yellow River	0.50	0.07	0.64	0.49 (0.98)	0.07 (0.94)	0.59 (0.92)	0.50 (1.01)	0.05 (0.73)	0.58 (0.90)

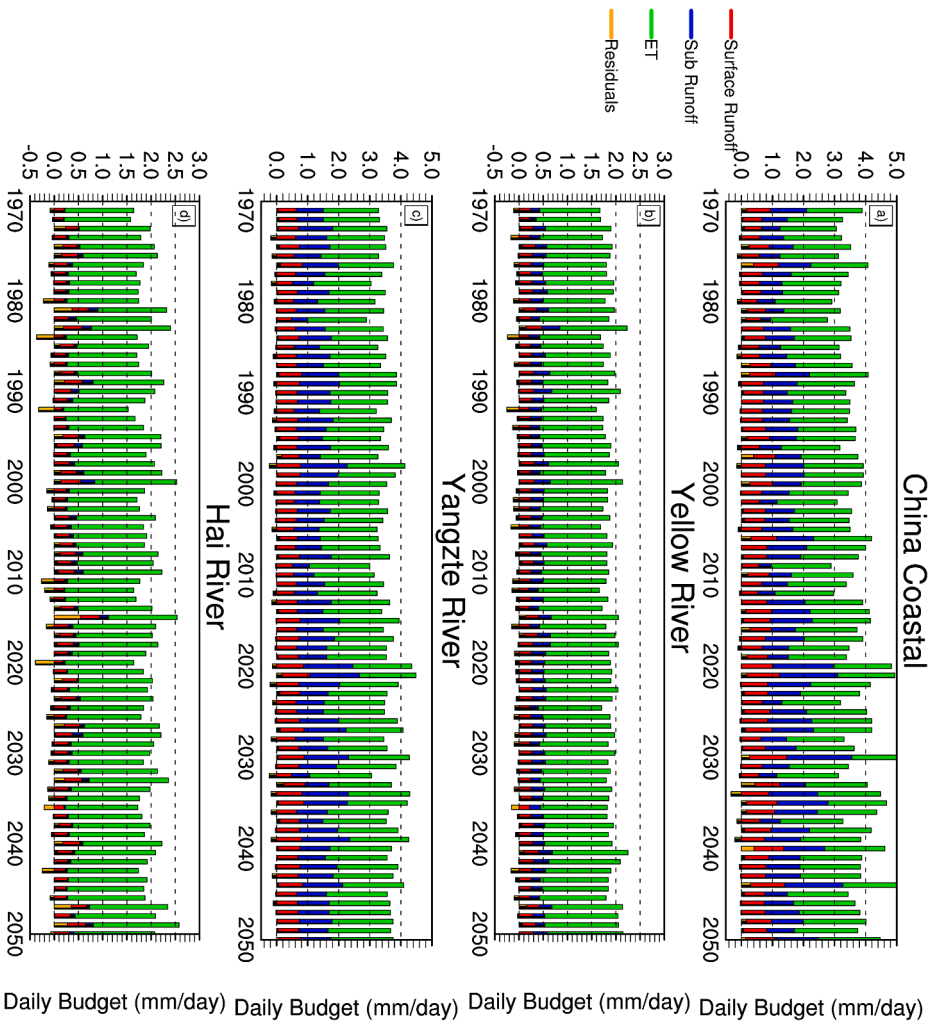

Fig. 11. Water budget of annual average precipitation, runoff and ET in the four regional-scale watersheds in China (China Coastal, Hai River, Yellow River, and Yangtze River) from 1970 to 2050. Residual = Precipitation - Runoff - ET.

CESM have the potential to be used for hydrological analysis at watershed scale, including the assessment of climate change impacts, the evaluation of extreme events, and quantification of the components in the water budget.

Declaration of Competing Interest

The authors declare that they have no known competing financial interests or personal relationships that could have appeared to influence the work reported in this paper.

Acknowledgments

This study is supported by the U.S. Department of Energy, Office of Science, Office of International Affair, U.S./China Clean Energy Research Center - Water/Energy Technologies (CERC-WET) project (award No. DE-IA0000018). This research used resources of the National Energy Research Scientific Computing Center (NERSC), a U.S. Department of Energy Office of Science User Facility located at Lawrence Berkeley National Laboratory, operated under Contract No. DE-AC02-05CH11231. The authors acknowledged the collaborations from Dr. Jie Zhang, Hongmei Xu and Chan Xiao, supported by the National Key Research and Development Program of China (Grant no. 2018YFE0196000). The authors also thank the associate editor and three anonymous reviewers' comments for improving the manuscript.

The VR-CESM simulations generated for this study are made available at the following NERSC Science Gateway: https://portal.nersc.gov/archive/home/z/zexuanxu/Shared/www/WUS_CHN_VRCESM14_historical. Please notify Zexuan Xu (zexuanxu@lbl.gov) if you access and use any of the VR-CESM datasets.

Appendix A. Supplementary data

Supplementary data associated with this article can be found, in the online version, at https://doi.org/10.1016/j.jhydrol.2021.126646.

References

Ackerley, D., Chadwick, R., Dommenget, D., Petrelli, P., 2018. An ensemble of amip simulations with prescribed land surface temperatures. Geoscientific Model Dev. 11, 3865–3881.

Ahl, R.S., Woods, S.W., Zuuring, H.R., 2008. Hydrologic calibration and validation of swat in a snow-dominated rocky mountain watershed, montana, usa 1. JAWRA J. Am. Water Resources Assoc. 44, 1411–1430.

Allen, P., Harmel, R., Dunbar, J., Arnold, J., 2011. Upland contribution of sediment and runoff during extreme drought: A study of the 1947–1956 drought in the blackland prairie, texas. J. Hydrol. 407, 1–11.

Archfield, S.A., Clark, M., Arheimer, B., Hay, L.E., McMillan, H., Kiang, J.E., Seibert, J., Hakala, K., Bock, A., Wagener, T., et al., 2015. Accelerating advances in continental domain hydrologic modeling. Water Resour. Res. 51, 10078–10091.

Arnold, J.G., Moriasi, D.N., Gassman, P.W., Abbaspour, K.C., White, M.J., Srinivasan, R., Santhi, C., Harmel, R., Van Griensven, A., Van Liew, M.W., et al., 2012. Swat: Model use, calibration, and validation. Trans. ASABE 55, 1491–1508.

Bales, R.C., Battles, J.J., Chen, Y., Conklin, M.H., Holst, E., O'Hara, K.L., Saksa, P., Stewart, W., 2011. Forests and water in the sierra nevada: Sierra nevada watershed ecosystem enhancement project. Sierra Nevada Research Institute report 11 http://ucanr.edu/sites/cff/files/146199.pdf.

Blöschl, G., Sivapalan, M., 1995. Scale issues in hydrological modelling: a review. Hydrological processes 9, 251–290.

Branstetter, M.L., & Famiglietti, J.S. (1999). Testing the sensitivity of gcm-simulated runoff to climate model resolution using a parallel river transport algorithm. In Preprints, 14th Conf. on Hydrology, Dallas, TX, Amer. Meteor. Soc (pp. 391–392).

Carroll, R.W., Gochis, D., Williams, K.H., 2020. Efficiency of the summer monsoon in generating streamflow within a snow-dominated headwater basin of the colorado river. Geophys. Res. Lett. 47 e2020GL090856.

Daly, C., Slater, M.E., Roberti, J.A., Laseter, S.H., Swift Jr, L.W., 2017. High-resolution precipitation mapping in a mountainous watershed: ground truth for evaluating uncertainty in a national precipitation dataset. Int. J. Climatol. 37, 124–137.

Dettinger, M.D., Anderson, M.L., 2015. Storage in California's Reservoirs and Snowpack in this Time of Drought. San Francisco Estuary and Watershed. Science 13, 1–5. https://doi.org/10.15447/sfews.2015v13iss2art1.

Du, E., Di Vittorio, A., Collins, W.D., 2016. Evaluation of hydrologic components of community land model 4 and bias identification. Int. J. Appl. Earth Observation Geoinformation 48, 5–16.

Foster, L.M., Bearup, L.A., Molotch, N.P., Brooks, P.D., Maxwell, R.M., 2016. Energy budget increases reduce mean streamflow more than snow–rain transitions: Using integrated modeling to isolate climate change impacts on rocky mountain hydrology. Environ. Res. Lett. 11, 044015.

Garousi-Nejad, I., He, S., Tang, Q., 2017. Comparison of coarse and high-resolution hydrologic modeling in mountainous areas. National Water Center Innovators Program Summer Institute Report 2017, (p. 14).

Gettelman, A., Bresch, D.N., Chen, C.C., Truesdale, J.E., Bacmeister, J.T., 2018. Projections of future tropical cyclone damage with a high-resolution global climate model. Climatic Change 146, 575–585.

Harbaugh, A.W., 2005. MODFLOW-2005, the US Geological Survey modular ground-water model: the ground-water flow process. US Department of the Interior, US Geological Survey Reston, VA.

Hayhoe, K., Cayan, D., Field, C.B., Frumhoff, P.C., Maurer, E.P., Miller, N.L., Moser, S.C., Schneider, S.H., Cahill, K.N., Cleland, E.E., et al., 2004. Emissions pathways, climate change, and impacts on california. Proc. National Acad. Sci. USA 101, 12422–12427. https://doi.org/10.1073/pnas.0404500101.

He, C., Chen, F., Barlage, M., Liu, C., Newman, A., Tang, W., Ikeda, K., Rasmussen, R., 2019. Can convection-permitting modeling provide decent precipitation for offline high-resolution snowpack simulations over mountains? J. Geophys. Res.: Atmospheres 124, 12631–12654.

Huang, X., Rhoades, A.M., Ullrich, P.A., Zarzycki, C.M., 2016. An evaluation of the variable-resolution cesm for modeling california's climate. J. Adv. Modeling Earth Systems 8, 345–369.

Hubbard, S.S., Williams, K.H., Agarwal, D., Banfield, J., Beller, H., Bouskill, N., Brodie, E., Carroll, R., Dafflon, B., Dwivedi, D., et al., 2018. The east river, colorado, watershed: A mountainous community testbed for improving predictive understanding of multiscale hydrological–biogeochemical dynamics. Vadose Zone J. 17, 1–25.

Hurrell, J.W., Hack, J.J., Shea, D., Caron, J.M., Rosinski, J., 2008. A new sea surface temperature and sea ice boundary dataset for the community atmosphere model. J. Clim. 21, 5145–5153. https://doi.org/10.1175/2008JCLI2292.1.

Khomsi, K., Mahe, G., Tramblay, Y., Sinan, M., Snoussi, M., 2016. Regional impacts of global change: seasonal trends in extreme rainfall, run-off and temperature in two contrasting regions of morocco. Natural Hazards Earth System Sci. 16, 1079–1090.

Lawrence, D.M., Oleson, K.W., Flanner, M.G., Thornton, P.E., Swenson, S.C., Lawrence, P.J., Zeng, X., Yang, Z.-L., Levis, S., Sakaguchi, K., et al., 2011. Parameterization improvements and functional and structural advances in version 4 of the community land model. J. Adv. Modeling Earth Syst. 3.

Lee, J., Xue, Y., De Sales, F., 2015. Spin-up simulation behaviors in a climate model to build a basement of long-time simulation. In: AGU Fall Meeting Abstracts, pp. A33J–0302 volume 2015.

Li, H., Huang, M., Wigmosta, M.S., Ke, Y., Coleman, A.M., Leung, L.R., Wang, A., Ricciuto, D.M., 2011. Evaluating runoff simulations from the community land model 4.0 using observations from flux towers and a mountainous watershed. J. Geophys. Res.: Atmospheres 116.

Li, H.-Y., Sivapalan, M., Tian, F., Harman, C., 2014. Functional approach to exploring climatic and landscape controls of runoff generation: 1. behavioral constraints on runoff volume. Water Resour. Res. 50, 9300–9322.

Lian, X., Piao, S., Huntingford, C., Li, Y., Zeng, Z., Wang, X., Ciais, P., McVicar, T.R., Peng, S., Ottle, C., et al., 2018. Partitioning global land evapotranspiration using cmip5 models constrained by observations. Nature Climate Change 8, 640–646.

Maina, F.Z., Siirila-Woodburn, E.R., Newcomer, M., Xu, Z., Steefel, C., 2020a. Determining the impact of a severe dry to wet transition on watershed hydrodynamics in california, usa with an integrated hydrologic model. J. Hydrol. 580, 124358.

Maina, F.Z., Siirila-Woodburn, E.R., Vahmani, P., 2020b. Sensitivity of meteorological-forcing resolution on hydrologic variables. Hydrol. Earth Syst. Sci. 24, 3451–3474.

Maraun, D., Widmann, M., 2018. Statistical downscaling and bias correction for climate research. Cambridge University Press.

Markstrom, S.L., Hay, L.E., Ward-Garrison, C.D., Risley, J.C., Battaglin, W.A., Bjerklie, D. M., 2009. Integrated watershed scale response to climate change for selected basins across the united states. Water Resources Impact 11, 8–10.

Massoud, E., Espinoza, V., Guan, B., Waliser, D., 2019. Global climate model ensemble approaches for future projections of atmospheric rivers. Earth's Future 7, 1136–1151.

Maxwell, R.M., Kollet, S.J., Smith, S.G., Woodward, C.S., Falgout, R.D., Ferguson, I.M., Baldwin, C., Bosl, W.J., Hornung, R., Ashby, S., 2009. Parflow user's manual. International Ground Water Modeling Center Report GWMI 1, 129.

Mishra, V., Shah, H.L., 2018. Hydroclimatological perspective of the kerala flood of 2018. J. Geol. Soc. India 92, 645–650.

Montavez, J.P., Lopez-Romero, J.M., Jerez, S., Gomez-Navarro, J.J., & Jimenez-Guerrero, P. (2017). How much spin-up period is really necessary in regional climate simulations? In EGU General Assembly Conference Abstracts (p. 15806).

Niu, G.-Y., Yang, Z.-L., Dickinson, R.E., Gulden, L.E., 2005. A simple topmodel-based runoff parameterization (simtop) for use in global climate models. J. Geophys. Res. Atmospheres, 110.

Nyunt, C.T., Koike, T., Yamamoto, A., 2016. Statistical bias correction for climate change impact on the basin scale precipitation in sri lanka, philippines, japan and tunisia. In: Hydrology and Earth System Sciences Discussions, pp. 1–32.

Oleson, K.W., Lawrence, D.M., Gordon, B., Flanner, M.G., Kluzek, E., Peter, J., Levis, S., Swenson, S.C., Thornton, E., Feddema, J. et al. (2010). Technical description of version 4.0 of the community land model (clm).

Rhoades, A.M., Ullrich, P.A., Zarzycki, C.M., 2018. Projecting 21st century snowpack trends in western usa mountains using variable-resolution cesm. Clim. Dyn. 50, 261–288.

Serreze, M.C., Clark, M.P., Armstrong, R.L., McGinnis, D.A., Pulwarty, R.S., 1999. Characteristics of the western united states snowpack from snowpack telemetry (snotel) data. Water Resour. Res. 35, 2145–2160.

Tesfa, T.K., Li, H.-Y., Leung, L., Huang, M., Ke, Y., Sun, Y., Liu, Y., 2014. A subbasin-based framework to represent land surface processes in an earth system model. Geoscientific Model Development 7, 947–963.

Ullrich, P. (2014). Squadgen: Spherical quadrilateral grid generator. University of California, Davis, Climate and Global Change Group software.[Available online at http://climate. ucdavis. edu/squadgen. php.].

Ullrich, P., Xu, Z., Rhoades, A., Dettinger, M., Mount, J., Jones, A., Vahmani, P., 2018. California's drought of the future: A midcentury recreation of the exceptional conditions of 2012–2017. Earth's Future 6, 1568–1587.

Velasquez, P., Messmer, M., Raible, C.C., 2020. A new bias-correction method for precipitation over complex terrain suitable for different climate states: a case study using wrf (version 3.8. 1). Geoscientific Model Dev. 13, 5007–5027.

Voisin, N., Liu, L., Hejazi, M., Tesfa, T., Li, H., Huang, M., Liu, Y., Leung, L., 2013. One-way coupling of an integrated assessment model and a water resources model: evaluation and implications of future changes over the us midwest. Hydrol. Earth Syst. Sci. 17, 4555.

Wu, C., Liu, X., Lin, Z., Rhoades, A.M., Ullrich, P.A., Zarzycki, C.M., Lu, Z., Rahimi-Esfarjani, S.R., 2017. Exploring a variable-resolution approach for simulating regional climate in the rocky mountain region using the vr-cesm. J. Geophys. Res.: Atmospheres 122, 10–939.

Xu, Z., Di Vittorio, A., Zhang, J., Rhoades, A.M., Xin, X., Xu, H., Xiao, C., 2021. Evaluating variable-resolution cesm over the western u.s. and eastern china for use in water-energy nexus and impacts modeling. J. Geophys. Res.: Atmospheres. https://doi.org/10.1029/2020JD034361. In press.

Xu, Z., Rhoades, A.M., Johansen, H., Ullrich, P.A., Collins, W.D., 2018. An intercomparison of gcm and rcm dynamical downscaling for characterizing the hydroclimatology of california and nevada. J. Hydrometeorol. 19, 1485–1506.

Yuan, X., Kaplan, M.R., Cane, M.A., 2018. The interconnected global climate system-a review of tropical–polar teleconnections. J. Clim. 31, 5765–5792.

Zarzycki, C.M., Jablonowski, C., Thatcher, D.R., Taylor, M.A., 2015. Effects of Localized Grid Refinement on the General Circulation and Climatology in the Community Atmosphere Model. J. Clim. 28, 2777–2803. https://doi.org/10.1175/JCLI-D-14-00599.1.

Zhao, T., Wang, Q.J., Schepen, A., Griffiths, M., 2019. Ensemble forecasting of monthly and seasonal reference crop evapotranspiration based on global climate model outputs. Agric. Forest Meteorology 264, 114–124.

Zhou, T., Leung, L.R., Leng, G., Voisin, N., Li, H.-Y., Craig, A.P., Tesfa, T., Mao, Y., 2020. Global irrigation characteristics and effects simulated by fully coupled land surface, river, and water management models in e3sm. J. Adv. Modeling Earth Systems 12 e2020MS002069.